Mass spectrometry of carbohydrate-protein interactions on a glycan array conjugated to CVD graphene surfaces

2D Materials

OPEN ACCESS

RECEIVED
22 September 2019

REVISED
26 November 2019

ACCEPTED FOR PUBLICATION
10 December 2019

PUBLISHED
6 January 2020

PAPER

Mass spectrometry of carbohydrate-protein interactions on a glycan array conjugated to CVD graphene surfaces

Juan Pedro Merino[1], Sonia Serna[2], Alejandro Criado[1], Alba Centeno[3], Ilargi Napal[3], Javier Calvo[4], Amaia Zurutuza[3], Niels Reichardt[2,5] and Maurizio Prato[1,6,7]

[1] Carbon Bionanotechnology Group, CIC BiomaGUNE, Parque Tecnológico de San Sebastián, Paseo Miramón, 182, 20014 San Sebastián, Guipúzcoa, Spain
[2] Glycotechnology Group, CIC BiomaGUNE, Parque Tecnológico de San Sebastián, Paseo Miramón, 182, 20014 San Sebastián, Guipúzcoa, Spain
[3] Graphenea S.A, Paseo Mikeletegi 83, 20009, San Sebastián, Spain
[4] Mass Spectrometry Lab, CIC BiomaGUNE, Parque Tecnológico de San Sebastián, Paseo Miramón, 182, 20014 San Sebastián, Guipúzcoa, Spain
[5] CIBER-BBN, Paseo Miramon 182, 20014 San Sebastián, Spain
[6] Department of Chemical and Pharmaceutical Sciences, Università degli Studi di Trieste, Via Licio Giorgieri 1, 34127 Trieste, Italy
[7] Basque Foundation for Science, Ikerbasque, 48013 Bilbao, Spain

E-mail: acriado@cicbiomagune.es, nreichardt@cicbiomagune.es and mprato@cicbiomagune.es

Keywords: graphene, CVD, chemical modification, LDI, mass spectrometry, carbohydrate microarrays, lectin

Supplementary material for this article is available online

Abstract

Mass spectrometry (MS) is a valuable tool for functional genomic, proteomic, and glycomic studies. In particular, the combination of MS with microarrays is a powerful technique for analyzing the activity of carbohydrate processing enzymes and for the identification of carbohydrate-binding proteins (lectins) in complex matrices. On the other hand, graphene exhibits high desorption/ionization efficiency, good conductivity and optical transparency, specifications of a high-performance component for matrix-assisted laser desorption/ionization (MALDI) platforms. Besides, the chemical functionalization of graphene increases the adsorption capability of functional biomolecules (e.g. receptors), resulting in very stable interfaces. Taking advantage of the properties of graphene, we developed several modified chemical vapor deposited graphene (CVDG)-based glycan arrays on different substrates including ITO and bare glass, as a potential sensing platform for carbohydrate-lectin interactions, which are involved in a plethora of biological processes. The glycan arrays were fully characterized by MALDI-MS analysis and, in some cases, optical microscopy.

1. Introduction

Graphene is a carbon material that presents a unique set of electronic, mechanical, optical, thermal and chemical properties [1]. The combination of these extraordinary properties qualifies graphene-based derivatives [2] as multifunctional materials for applications in sensing, energy storage, optoelectronic devices, as catalyst supports, and as composites in the development of new analytical tools [3].

Matrix-assisted laser desorption/ionization time-of-flight (MALDI-TOF) mass spectrometry (MS) provides a simple and high-throughput method of analysis for biomolecules [4–6] that stands out for its speed, robustness and ease of handling.

With the introduction of nanomaterials into this analytical tool, a significant improvement was achieved for the analysis of complex samples [7, 8]. Particularly, they can address the issues in MALDI-TOF MS related to low reproducibility in matrix crystallisation, hot spot formation and matrix ion interference in small molecule analysis [5]. Oxidized graphene related materials have been widely employed as matrix for the detection of molecules with low molecular weight, metal ions, and biomolecules such as lipids, proteins and carbohydrates by laser desorption ionisation mass

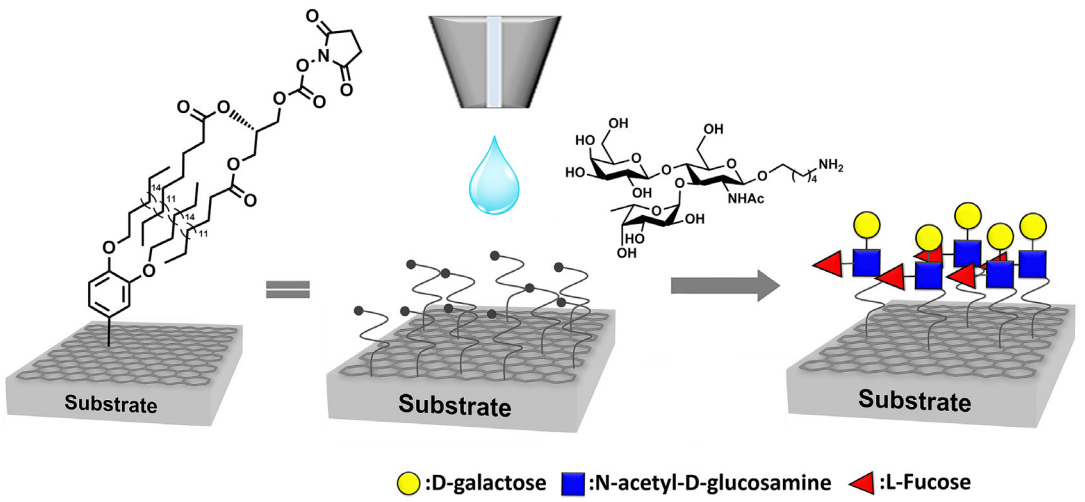

Figure 1. General representation of preparation of CVDG-based carbohydrate microarrays for dual MS and optical microscopy readout. As example, Lewis^x carbohydrate structure is represented.

spectrometry (LDI-MS). Recently, with graphene oxide (GO) as matrix, researchers were able to detect more than two hundred molecules, including lipids and metabolites by LDI-MS, and employed the nanomaterial for the *in situ* MALDI-imaging of mouse brain tissue sections [9]. In addition, graphene presents a high binding capability towards aromatic compounds, which can serve as an enrichment method improving analysis efficacy [10]. For interaction assays, however, the noncovalent arbitrary analyte deposition could prove problematic and decrease assay sensitivity and reproducibility.

A wide range of semiconductor, metal and carbon materials have been studied as sample supports for the matrix-free LDI-MS [11–18]. For LDI-MS an ideal substrate should present the following features: (1) efficient laser absorption and electrical conductivity with high electron mobility for optimal ionization; (2) stable under laser irradiation to avoid interferences with analyte; (3) homogeneous and large surface area with good interaction with analyte molecules for reproducibility and accurate analysis. To the best of our knowledge, there are few examples referring to graphene derivative-coated surfaces for surface assisted matrix assisted laser desorption/ionization (SALDI) MS, all based on GO derivatives [14, 15, 19, 20]. For instance, a reduced GO paper as a substrate for matrix-free LDI-MS detection significantly increased the detection limit of diverse molecules compared to commercial products [14]. In addition, a GO-doped resin target fabricated via 3D-printing for LDI-MS has been recently reported [19]. The GO doped in the target acts as laser absorber and ionization promoter, thus permitting the direct analysis of samples without addition of an organic matrix.

However, current substrates are far from ideal in terms of stability, reproducibility and effective functionalization; thus, improved performance with new materials is demanded. In addition, the manufacture of multiplex detection devices is an attractive strategy for the design of sensitive and selective sensing platforms. In particular, chemical vapour deposited graphene (CVDG) is a promising but largely unexplored candidate for these applications.

Graphene can be covalently or non-covalently modified by a range of functional groups including carboxylic acid, hydroxyl, amine and azide groups as handles for further modifications [21–23]. The activation of graphene with reactive groups has the advantage of providing oriented analyte immobilization and concomitant passivation of the surface, to avoid unspecific adsorption of contaminants that could interfere in the analysis. In this context, an improvement of the standard MALDI method for the detection of N-glycans released from glycoproteins was reported by using noncovalent functionalized GO via π–π stacking interactions with pyrene derivatives activated as acid chlorides [24]. The non-covalent immobilization of carbohydrates on graphene and carbon nanotubes via the formation of pyrene and porphyrin based glycoconjugates has also been applied in the electronic detection of bacterial virulence factors from *Pseudomonas aeruginosa* [25].

Here, we report the use of CVDG as a platform for the preparation of glycan arrays to monitor carbohydrate-lectin interactions by MS and fluorescence (figure 1). CVDG seemed an ideal material for this purpose as it combines properties such as high surface area, chemical modification capability to immobilize receptors, high conductivity required for the MS detection, and high transparency to detect interactions via fluorescence readout [3].

2. Results and discussion

The glycan array reported here is based on glass slides coated with functionalized CVDG. This graphene derivative is a conductive material with high

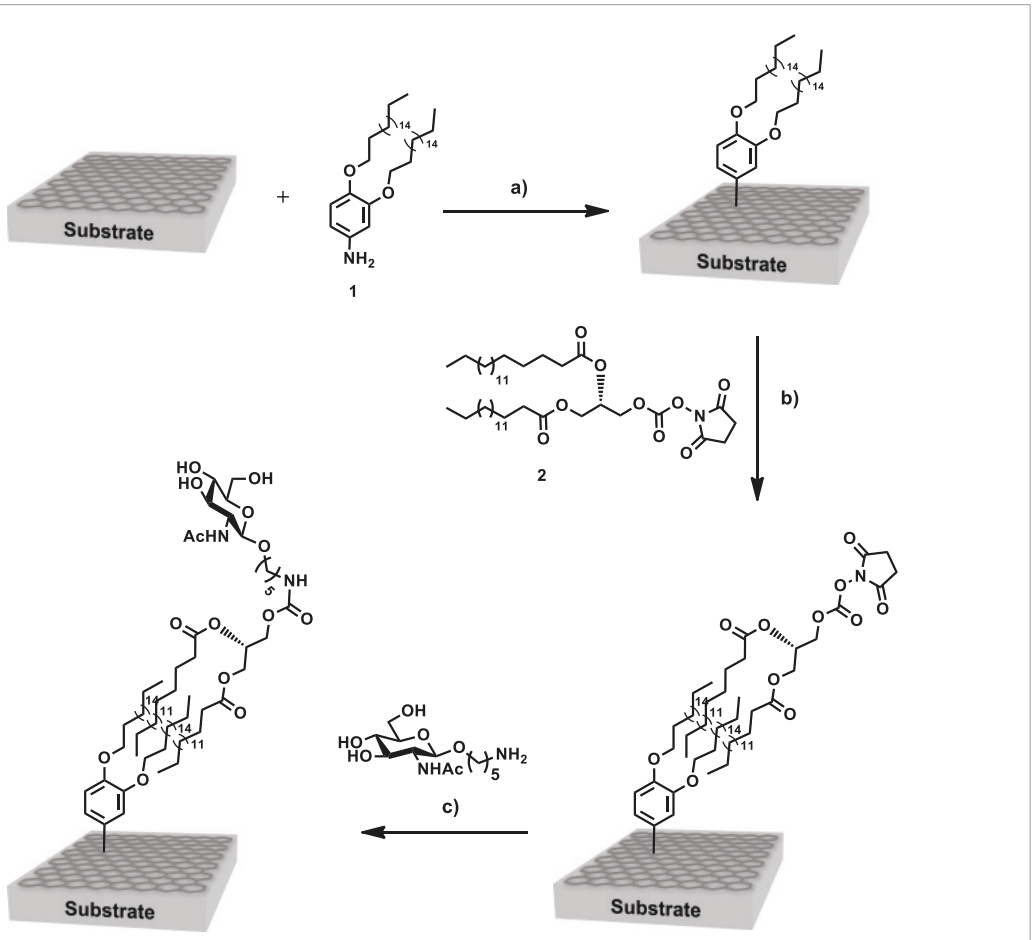

Scheme 1. Functionalization of CVDG substrates. Reagents and conditions: (a) **1** (1 equiv), 3-methylbuthylnitrite (1.5 equiv), 60 °C; (b) **2** (1 mM) in $CHCl_3$, RT, overnight; (c) 5-aminopentyl carbohydrates (100 μM), sodium phosphate buffer 300 mM pH = 8.5, RT, overnight. As example, structure of 5-aminopentyl GlcNAc carbohydrate is represented.

electron mobility, good optical properties, showing a transmittance of 97% [26]; homogeneous surface and easily functionalized with the affinity ligand of interest. A combination of covalent and non-covalent functionalization of graphene was required to desorb the immobilised ligands and to allow the preparation of functional structures with high chemical stability and under tight process control. Two types of transparent materials were addressed: (1) conductive and well-characterized ITO-coated glass; and (2) non-conductive non-coated soda lime glass slides. Firstly, CVDG was included into a previously reported glycan microarray format by the deposition of CVDG on ITO-coated glass [27]. We expected to raise the sensitivity of the well-established method by taking advantage of the intrinsic properties of graphene using ITO-coated glass as supporting substrate. While surface parameters as transparency, surface area, fragmentation capacity and potential for chemical modification are readily explored on the ITO-coated glass surfaces, the indium tin oxide coating interfered in the measurement of graphene based electrical conductivity, which was assessed on bare glass microscope slides.

2.1. Preparation of carbohydrate microarrays on CVDG

In general terms, the functionalization of a graphene-based microarray was based on the formation of a hydrophobic bilayer via the combination of covalent and non-covalent modification of graphene (Scheme 1). Initially, the graphene surface was covalently functionalized with stearyl alkoxide-substituted aniline derivative **1** via a diazonium salt reaction [28] and further modified by hydrophobic interactions with the N-hydroxysuccinimide (NHS) activated bidentate 1,2-*sn*-dipalmitoyl glycerol **2**. Onto this NHS activated hydrophobic bilayer, amine-containing ligands can be robotically printed and immobilized as highly stable carbamates. In addition, the terminal reactivity of the bidentate linker might be easily changed to azide, alkyne [29] or amine groups to accommodate other ligand types. Hereupon, *p*mol amounts of 5-amino-pentyl

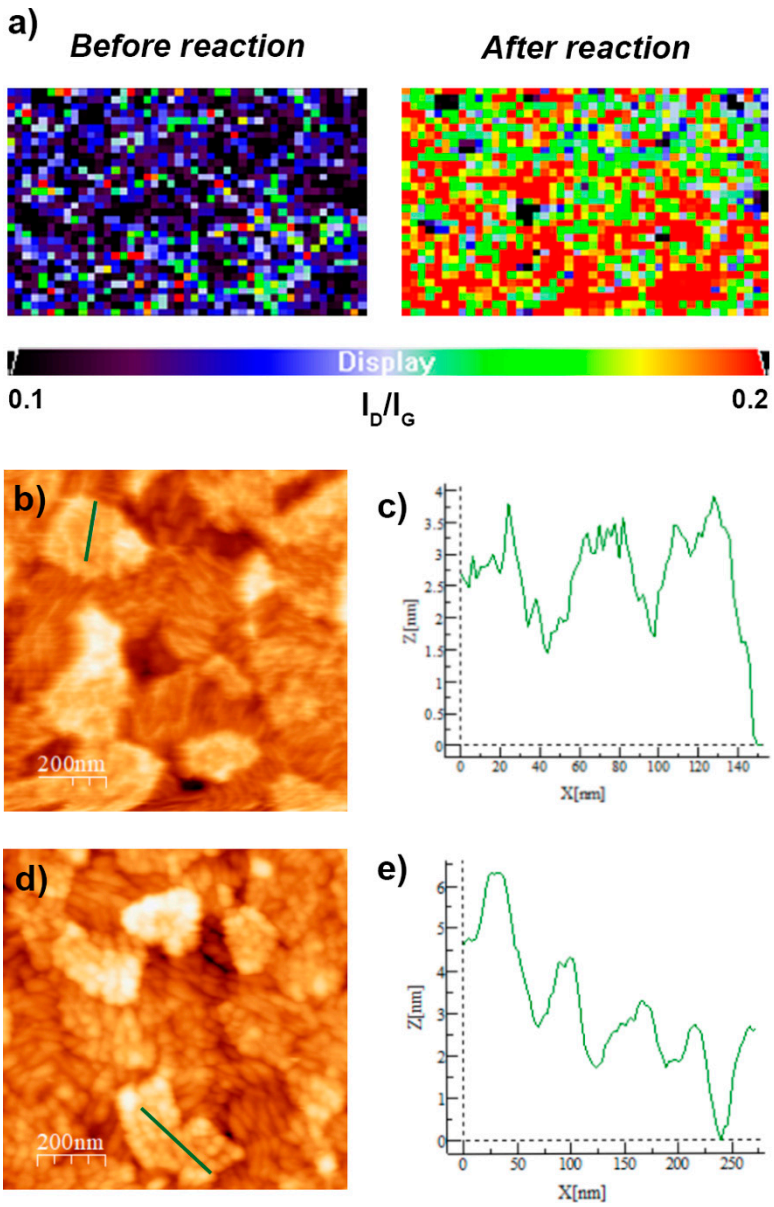

Figure 2. (a) Raman mapping of the D band intensity in 30 × 25 μm^2 graphene area before and after covalent modification of CVDG on ITO-coated glass. AFM image ((b) and (d)) and AFM height profile ((c) and (e)) of CVDG on ITO-coated glass before ((b)–(c)) and after ((d) and (e)) covalent modification.

modified carbohydrates were spatially arrayed on the different surfaces, generating micrometer sized spots of the immobilized carbohydrates.

2.1.1. Covalent modification of pristine graphene

In a proof of concept experiment, we studied the covalent modification of CVDG with the diazonium salt generated from aniline **1** on SiO_2 and characterized the resulting surface by Raman spectroscopy and AFM (see supporting information). Pristine CVDG on SiO_2 measured with a 532 nm excitation laser showed the characteristic G, D and 2D bands at 1350, 1580 and 2700 cm^{-1}, respectively (figures S5(a) and (b) (stacks.iop.org/TDM/7/024003/mmedia)). After treatment with the *in situ* generated diazonium salt from the aniline **1**, the graphene surface showed a slight increment of the D band ($\Delta(I_D/I_G) = 0.05$, figure S5(b)). This increased intensity might be explained by the formation of structural sp^3 defects in the graphene structure where the corresponding functional groups are covalently attached. This covalent modification, tends to produce a low number of defects (low I_D/I_G ratio) in order to preserve the intrinsic properties of CVDG [30, 31]. Interestingly, AFM showed significant changes in the surface morphology, probably due to the well-known oligomers derived from the generated phenyl radicals (figure S6) [32]. For improved clarity we depict the attachment of a 3,4-octadeciloxi-phenyl monomer on the graphene surface (Scheme 3) but, probably, oligomers derived from 3,4-octadeciloxi-phenyl radicals are obtained and immobilized (figure S7).

After confirming the covalent modification of CVDG on a generic substrate, the preparation of the different graphene-based microarray platforms were addressed. Consequently, CVDG on ITO-coated glass

Table 1. MS detection of different immobilized carbohydrates using CVDG-based substrates by MALDI-TOF.

		ITO/CVDG		Bare glass/CVDG	
Carbohydrate	*m/z* $[M+Na]^+$	Peak intensity	*S/N*	Peak intensity	*S/N*
GlcNAc	923.65	3525	292.1	5292	736.4
LacNAc	1085.71	3281	743.5	2016	385.3
Lactose	1044.68	2587	365.0	1577	276.2
Le^x	1231.76	2783	271.2	2789	417.1

and uncoated glass slides were covalently functionalized and characterized by Raman spectroscopy, x-ray photoelectron spectroscopy (XPS) analysis, water contact angle measurements and AFM. Raman mapping studies of areas around $30 \times 20\ \mu m^2$ for graphene on ITO-coated glass showed an increment of D and D′ band at 1350 and 1615 cm^{-1}, respectively (figures 2(a) and S5(c), (d)). In addition, XPS analysis of the chemical composition of the graphene surface was performed to provide evidence of the graphene functionalization. The XPS analysis showed an increase of atomic carbon concentration after functionalization (table S1). Focusing on the atomic carbon composition, pristine graphene substrates showed a C1s core level composed of graphenic C = C asymmetric component (284.37 eV) and oxygenated carbon groups such as C–O and C=O components (~286 and ~288 eV, respectively; table S2). However, after covalent functionalization, C = C/C–C component in the C1s core level significantly increased, probably because of the introduction of the dialkoxyphenyl moieties. In order to determine the influence of the functionalization on the surface hydrophobicity, the water contact angle was measured (figures S14(a)–(c)). The contact angle on functionalized graphene on ITO-coated glass was slightly increased with respect to the pristine material, probably, due to the introduction of alkane chains. In addition, the surface morphology was studied by AFM after functionalization and a thorough washing process. The AFM images of functionalized graphene on ITO-coated glass suggested the existence of an amorphous layer on the surface composed of a significant fraction of aryl oligomers (figures 2(b)–(d) and S8) [32].

On the other hand, the characterization of covalently modified CVDG on bare glass showed only a low increment in the D band ($\Delta(I_D/I_G) = 0.01$, figure S5(f)) by Raman spectroscopy. XPS analysis confirmed the expected increment in the C = C/C–C component (284.37 eV), due to the presence of phenyl oligomers (table S2). Nevertheless, the contact angle measurements and the morphology study by AFM for functionalized graphene on bare glass were not conclusive due to the high roughness of the glass substrate (figure S9). Overall, characterizing CVDG on bare glass was quite challenging, due to the poorer surface characteristics of bare glass as compared to ITO coatings.

2.1.2. Non-covalent modification of covalently modified graphene

After the covalent modification, the immobilization of N-hydroxysuccinimide (NHS) activated bidentate 1,2-*sn*-dipalmitoyl glycerol linker was carried out onto ITO/CVDG and glass/CVDG modified graphene substrates. To evaluate the adsorption of the lipidic bidentate linker MALDI-TOF MS after matrix deposition was carried out and the immobilization could be clearly confirmed on both CVDG-based substrates (figure S15). The activation of the surface with reactive NHS groups permits the immobilization of amine containing biomolecules. Then, as a proof of concept, solutions (15 nl) of 5-aminopentyl modified carbohydrates (figure S16(a)): N-acetyl-D-glucosamine (**GlcNAc**), N-acetyl-D-lactosamine (**LacNAc**), lactose (**Lac**) and Lewis^x trisaccharide (**Le^x**) were robotically dispensed on both NHS activated substrates. Each spot contains *p*mol amounts of each carbohydrate forming subarrays of four different carbohydrates each of them printed in five replicates (figure S16(b)). All hydrophobic bilayers showed high stability during aqueous washings and excess of buffers or reagents in the printing solutions could be removed by a simple washing procedure. Non-reacted NHS groups were quenched by the immersion of the substrates in ethanolamine solution.

The successful immobilization of the carbohydrates was monitored by MALDI-TOF MS after matrix deposition. Under laser irradiation, the hydrophobic bilayer is disrupted allowing the detection of carbohydrates coupled to bidentate linker on individual spots. For an accurate comparison of the different CVDG substrate performance, all spectra were recorded under identical laser settings and power conditions and a sum of 500 shots was acquired in each spectrum. Both ITO/CVDG and glass/CVDG showed similar performance in the analysis of immobilized carbohydrates (table 1). Clean, mass spectra with high ion intensity and good signal to noise ratio were obtained from individual spots (figures 3(a) and (b)). The performance of CVDG-glass microarrays was compared with previously described hydrophobic coated ITO based microarrays [27]. CVDG coated glass slides showed a similar performance as the C-18 alkane coated ITO microarrays (figure S17 and table S3) Therefore, CVDG-glass could become an alternative to the use of ITO-coated glass in carbohydrate microarray fabrication.

In addition, carbohydrates immobilized on glass/CVDG microarrays were efficiently detected under matrix-free conditions (figure 3(c)). Thus, the role of graphene as a SALDI platform was confirmed. As graphene surfaces show high hydrophobicity (figures S14(b) and (e)) and their interaction with phospholipids has been previously described [33],

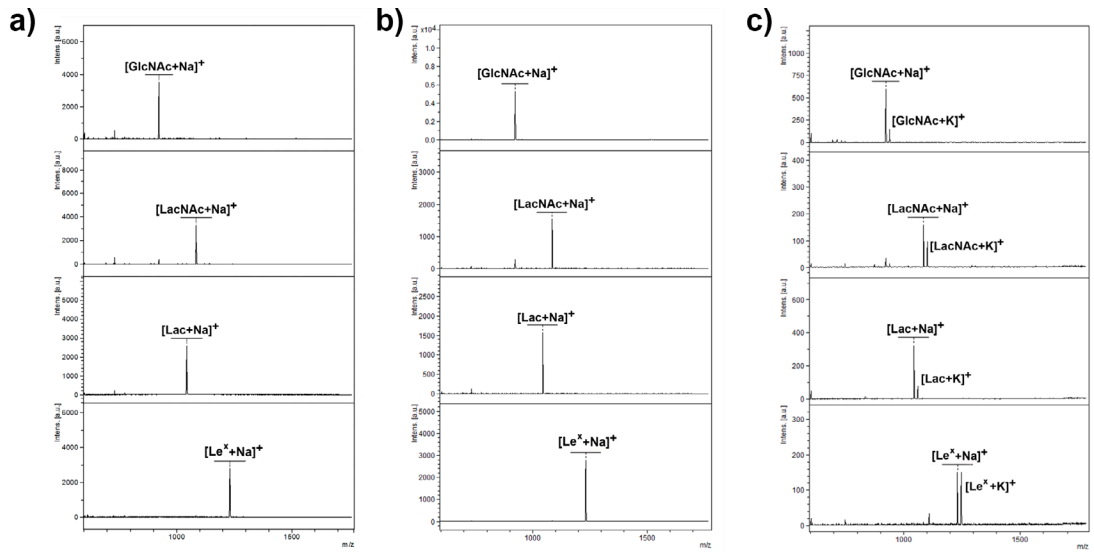

Figure 3. Mass spectra of carbohydrates immobilized on ITO/CVDG (a), and on glass/CVDG microarrays (b) by MALDI-TOF using DHB as matrix. (c) Mass spectra of carbohydrates immobilized on glass/CVDG microarrays by matrix-free LDI.

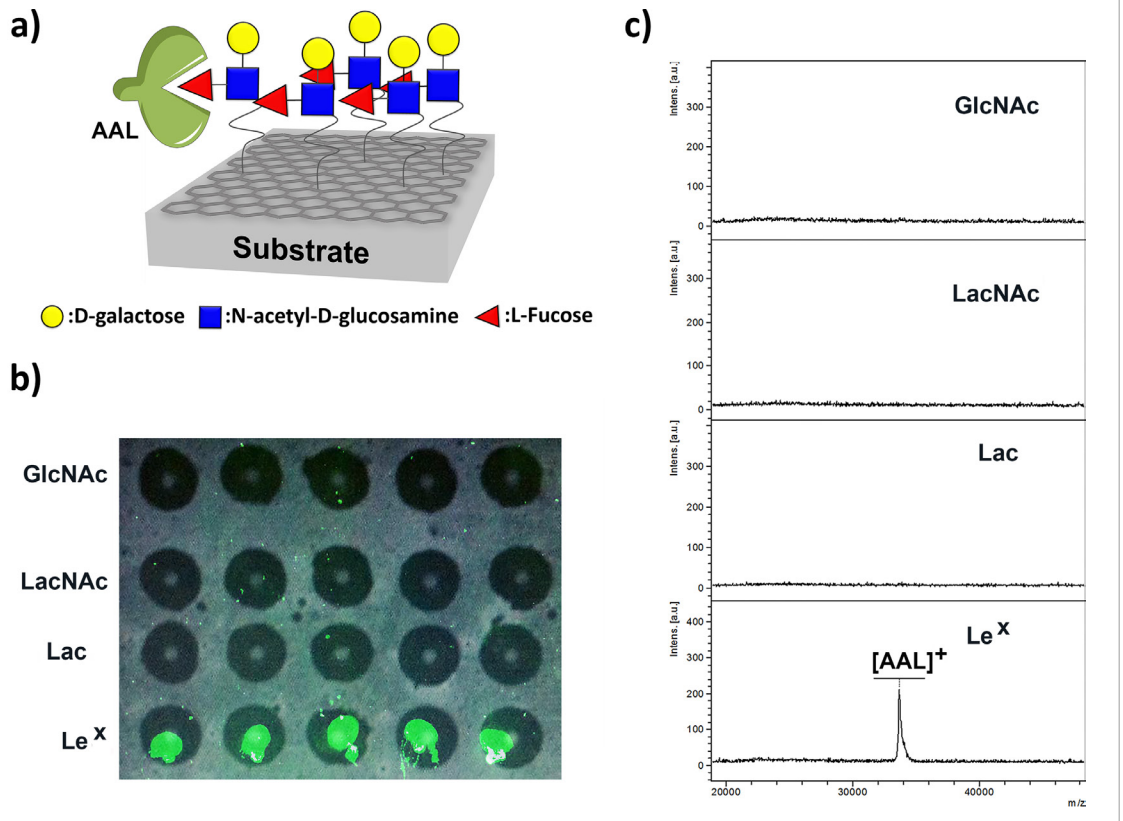

Figure 4. Detection of carbohydrate binding proteins (lectins) on CVDG microarrays. (a) Schematic representation of *Aleuria aurantia* lectin (AAL) binding towards fucosylated **Le^x** structure. (b) Fluorescence detection of AAL-555 binding towards Le^x. Figure shows the superimpose image of printed drops and the fluorescence emission of AAL-555 measured by microarray scanner. (c) Detection of AAL binding towards **Le^x** by MALDI-TOF MS.

we evaluated the assay performance for arrays with the bidentate activated linker **2** directly immobilized on the non-derivatized CVDG surface. MS spectra recorded under identical conditions showed that the direct neoglycolipid immobilization on graphene surface produced spectra with far lower S/N and spectral quality than spectra obtained from graphene, which had been hydrophobically derivatised with the dialkoxy aniline ligand **1** (figure S18 and table S4).

This experimental evidence suggests that the covalent hydrophobic modification of the graphene layer, although does not affect substantially the hydrophobic

properties of the material, can lead to a higher loading of the bidentate linker **2** and consequently to an increase in the loading of immobilized carbohydrates.

2.2. Detection of carbohydrate-lectin interactions

Next, the detection of carbohydrate-lectin interactions on CVDG-based microarrays was explored (figure 4(a)). Lectins are proteins that recognize specific structural elements of carbohydrates with high selectivity, acting as translators of the information encoded by carbohydrates on the cell surface or in extracellular proteins. Lectins are widespread in all living organisms, from bacteria to mammals and display numerous biological functions, in cell–cell communication, fertilization and immune response, e.g. through the recognition of foreign carbohydrates presented in colonizing pathogens [34]. Carbohydrate microarrays have been extensively employed as high throughput screening tools for the characterization of these proteins [35, 36]. Commonly, carbohydrate-lectin interactions on microarrays are quantified via the emitted fluorescence of the adhered labelled lectins after a washing step to remove non-binders. It is well documented that graphene can quench fluorescent dyes via fluorescence resonant energy transfer (FRET) with high efficiency. In fact, bioassays based on the quenching and subsequent recovery of the fluorescence on graphene has been developed to study carbohydrate-lectin interactions [37, 38].

We hypothesized that the hydrophobic bilayer constructed on CVDG based microarrays could provide enough distance to avoid FRET based quenching of the dyes allowing fluorescence measurements on these surfaces. To verify this hypothesis, we incubated CVDG carbohydrate microarrays with fluorescently labelled lectin *Aleuria aurantia* (AAL). AAL is isolated from orange peel fungus and recognizes L-fucose, with a broad specificity towards different linkages (α-1,2; α-1,3; α-1,4; α-1,6-). This lectin is commonly employed as a tool in the isolation and characterization of fucosylated glycoproteins which are often overexpressed in different types of cancers [39]. After incubation with AAL-555, the glass/CVDG carbohydrate microarray was washed and scanned in a microarray scanner (figure 4(b)). Fluorescence was only observed for spots corresponding to the immobilized **Le^x** carbohydrate, which was the only fucosylated structure on the array. Additionally, the label-free detection of carbohydrate-lectin interactions by MS was studied [40]. After incubation of array prepared on glass/CVDG with AAL solution, we could detect by MALDI-TOF MS a peak at $m/z = 33\,691$ Da $[AAL]^+$ [41] corresponding to the monomeric lectin exclusively on spots of immobilized **Le^x** carbohydrate (figure 4(c)).

3. Conclusions

In conclusion, we have studied the preparation of MS active CVDG carbohydrate microarrays on a variety of supporting materials. The construction of NHS active surfaces on CVDG was based on the formation of a hydrophobic bilayer on chemically derivatized graphene. The presence of the bilayer was required for an effective mass detection of the immobilized analytes. Low cost materials such as uncoated microscope glass slides were sufficient as surface for CDVG deposition and the subsequent functionalization for the preparation of microarrays without the need of an ITO adhesive layer.

The potential of CVDG as a performance component for LDI-MS analysis is reported for the first time. In particular, CVDG behaved as anchoring platform on ITO and as conductive surface on bare glass substrates for matrix-free LDI. Likewise, the crucial role of chemical functionalization for the manufacture of CVDG carbohydrate microarrays was established.

We speculate that this methodology might be further expanded with the immobilization of other biomolecules such as DNA, peptides or proteins for the development of LDI-MS-based assays [42]. The dual readout could aid in the discovery and assignment of new carbohydrate binding proteins and antibodies from complex biofluids. More broadly speaking our array platform could have interesting new applications in the characterization of biomolecules in their native environments as both affinity measurements and identification could be achieved in a single platform. So, we foresee applications both in the discovery and characterization of disease biomarkers and as diagnostic tools, for example in the early identification of bacteria from biological fluids.

4. Experimental section

4.1. General

Chemicals were acquired from Merck and were used as received. Raman spectra were collected on a Renishaw Invia Raman microspectrometer comprised of a laser source at 532 nm wavelength, a high-resolution diffraction grafting of 1800 g mm^{-1} and a Peltier-cooled front-illuminated CCD camera. XPS spectra were obtained using a SPECS Sage HR 100 spectrometer with a nonmonochromatic x-ray source of Aluminium with a Kα line (1486.6 eV, 300 W). XPS data was analyzed with CasaXPS software. Surface topologies of slides were characterized by AFM (JPK NanoWizard II) in intermittent contact tapping mode. A tapping etched silicon probe (TESPA-V2) with a 0.01–0.025 Ω/cm antimony (n) doped Si was employed, equipped with a rectangular cantilever: (3.8 μm thickness, nominal resonant frequency of 320 kHz, spring constant of 42 N/m, length of 123 μm, and width of 40 μm). The AFM-images were analyzed employing WSxM 5.0 Develop 7.0 software. For mass analysis, the spectra were obtained on a Bruker Ultraflextreme III TOF mass spectrometer and the data was acquired using the FlexControl 3.3 software (Bruker Daltonics, Bremen, Germany). The spectrophotometer was

equipped with a pulsed Nd:YAG laser ($\lambda = 355$ nm). 5000 shots per spectrum were acquired in positive reflector or positive linear ion mode (pulse duration of 50 ns, a 40 frequency of 1000 Hz, a laser fluence of 30%, laser focus settings: offset = 0%, range = 100%, and value = 9.5%). The *m*/*z* range was chosen according to the mass of the analyte. The spectra were processed with FlexAnalysis v3.3 software. For calibration of mass spectra INTAVIS peptide calibration standard mixture II was employed.

Microarrays were prepared with a SciFLEXARRAYER piezoelectric spotter S11 (Scienion, Berlin, Germany). Fluorescence images were obtained on a microarray scanner system (Agilent G265BA, Agilent Technologies, Santa Clara, USA).

All slides employed have the dimensions of 75 mm × 25 mm. ITO coated slides (ITO thickness of 130 nm) were purchased from Hudson Surface Technology, Inc. (Fort Lee, NJ), with a nominal transmittance of >78%. Glass microscope slides (thickness 0.96–1.06 mm) were acquired from Corning Incorporated (Corning, NY).

Both ITO and bare glass slides were cleaned by immersion in piranha solution (H_2O:H_2O_2:NH_3, 40:15:15 ml) for 1 h at 60 °C before CVDG coating.

The high quality monolayer graphene was grown in a cold wall CVD reactor (4″ Aixtron BM). Then, CVD monolayer graphene was transferred to ITO-coated glass or bare glass substrates by using poly(methyl methacrylate) (PMMA) assisted wet transfer process. 100 nm of PMMA were spin-coated on top of graphene/copper samples followed by chemical etching of the graphene bottom layer. Afterwards the copper catalyst was etched away with ferric chloride for 90 min and cleaned with distilled water using a semi-automatic system. Finally, the supported polymer was removed by dipping in acetone and isopropanol for 30 min each bath and dried in a hotplate at 150 °C.

1,2-Dipalmitoyl-*sn*-glycerol was treated with *N*,*N*′-disuccinimidyl carbonate to produce **2**, as previously reported [27]. *Aleuria aurantia* lectin was provided by Vector laboratories (Burlingame, CA, USA) and labelled with Alexa Fluor™ 555 NHS succinimidyl ester from Thermo Fischer following manufacturer instructions.

4.2. Covalent modification of CVDG

3,4-bis(octadecyloxy)aniline (**1**, 403 mg, 0.64 mmol) was placed in a flask previously purged with argon and dissolved in dry DMF (80 ml) under sonication. Then, the graphene substrate was introduced in the flask and 3-methylbuthylnitrite (129 μl, 0.96 mmol) was slowly added dropwise. The resulting mixture was heated to 60 °C and left without stirring for 2 h. The substrate was removed from the reaction mixture and cleaned by immersion in toluene for 12 h and in EtOH for 30′. The modified graphene substrate was dried over a stream of N_2.

4.3. Bilayer preparation

Modified graphene slide was incubated overnight at r.t. with (S)-3-((2,5-dioxocyclopentyloxy)carbonyloxy) propane-1,2-diyl dipalmitate (**2**, 1 mM solution in $CHCl_3$). The slide was left to dry under ambient conditions and stored at -20 °C or under vacuum.

4.4. Carbohydrate printing and analysis by MALDI-TOF

Solutions (100 μM) of C5-amino linked carbohydrates (**GlcNAc**, **LacNAc**, **Lac** and **Le^x**) in phosphate buffer (300 mM, pH 8.5) were robotically printed (50 droplets, ≈ 15 nl, ≈ 1.7 pmol) onto slides functionalized with activated bidentate linker at a pitch of 750 μm in both *x* and *y*-directions, and left to react overnight at r.t. and controlled humidity of 90%. The slides were quenched by immersion in ethanolamine solution (50 mM) in sodium borate buffer (50 mM, pH = 9.0).

For matrix assisted MS analysis, 2,5- dihydroxibenzoic acid (DHB) matrix (15 nl of 4 mg/ml in water:acetonitrile, 90:10 containing 0.1% trifluoroacetic acid (TFA) and 0.005% of NaCl) was spotted on top of the carbohydrates and then crystallized prior to MALDI-TOF measurements.

4.5. Lectin incubation

Subarrays were compartmentalized using 8-well ProPlate® incubation chambers from GraceBiolabs and treated with *Aleuria aurantia* lectin (AAL). A solution containing AAL-555 or unconjugated AAL (50 μg/ml) in Hepes buffer (50 mM, pH = 8.0) was incubated at room temperature for one hour. Before removing the incubation chamber the subarrays were washed sequentially with Hepes buffer and water. The complete slides were washed by immersion in water and dried under a stream of argon. For fluorescence measurements the slide was scanned in Agilent G265BA microarray scanner.

For MALDI-TOF mass detection of AAL a solution (15 nl) containing a mixture 1:1 of DHB solution and α-cyano-4-hydroxycinnamic acid (α-CHCA) matrix solution (4 mg/ml in water:acetonitrile 70:30 containing 5% formic acid) was spotted on top of the printed carbohydrates allowed to crystallize prior to MALDI-TOF measurements.

Acknowledgments

M Prato is the recipient of the AXA Chair (2016-2023). A Criado thanks MINECO to his research grant (Juan de la Cierva—Incorporación). This work was supported by the European Union's Horizon 2020 research and innovation program under Grant Agreements 696656 and 785219 Graphene Flagship. Funding from the Spanish Ministry of Economy, Industry and Competitiveness (project CTQ2016-76721-R to M Prato and Grant CTQ2017-90039-R to N-C Reichardt) is acknowledged. This work was

performed under the Maria de Maeztu Units of Excellence Program from the Spanish State Research Agency—Grant No. MDM-2017-0720.

ORCID iDs

Juan Pedro Merino https://orcid.org/0000-0002-3260-4947
Sonia Serna https://orcid.org/0000-0002-2085-4412
Alejandro Criado https://orcid.org/0000-0002-9732-513X
Alba Centeno https://orcid.org/0000-0001-8442-2283
Niels Reichardt https://orcid.org/0000-0002-9092-7023
Maurizio Prato https://orcid.org/0000-0002-8869-8612

References

[1] Novoselov K S, Geim A K, Morozov S V, Jiang D, Zhang Y, Dubonos S V, Grigorieva I V and Firsov A A 2004 Electric field effect in atomically thin carbon films *Science* **306** 666–9
[2] Wick P *et al* 2014 Classification framework for graphene-based materials *Angew. Chem., Int. Ed. Engl.* **53** 2–7
[3] Ferrari A C *et al* 2015 Science and technology roadmap for graphene, related two-dimensional crystals, and hybrid systems *Nanoscale* **7** 4598–810
[4] Su J and Mrksich M 2002 Using mass spectrometry to characterize self- assembled monolayers presenting peptides, proteins, and carbohydrates *Angew. Chem., Int. Ed. Engl.* **41** 4715–8
[5] Mandal A, Singha M, Addy P S and Basak A 2019 Laser desorption ionization mass spectrometry: recent progress in matrix-free and label-assisted techniques *Mass Spectrom. Rev.* **38** 3–21
[6] Leopold J, Popkova Y, Engel K M and Schiller J 2018 Recent developments of useful MALDI matrices for the mass spectrometric characterization of lipids *Biomolecules* **8** 173
[7] Wang J, Liu Q, Liang Y and Jiang G 2016 Recent progress in application of carbon nanomaterials in laser desorption/ ionization mass spectrometry *Anal. Bioanal. Chem.* **408** 2861–73
[8] Lu M, Yang X, Yang Y, Qin P, Wu X and Cai Z 2017 Nanomaterials as assisted matrix of laser desorption/ ionization time-of-flight mass spectrometry for the analysis of small molecules *Nanomaterials* **7** 87
[9] Zhou D, Guo S, Zhang M, Liu Y, Chen T and Li Z 2017 Mass spectrometry imaging of small molecules in biological tissues using graphene oxide as a matrix *Anal. Chim. Acta* **962** 52–9
[10] Shi C, Meng J and Deng C 2012 Enrichment and detection of small molecules using magnetic graphene as an adsorbent and a novel matrix of MALDI-TOF-MS *Chem. Commun.* **48** 2418–20
[11] Picca R A, Calvano C D, Cioffi N and Palmisano F 2017 Mechanisms of nanophase-induced desorption in LDI-MS. A short review *Nanomaterials* **7** 75
[12] Shi C Y and Deng C H 2016 Recent advances in inorganic materials for LDI-MS analysis of small molecules *Analyst* **141** 2816–26
[13] Silina Y E and Volmer D A 2013 Nanostructured solid substrates for efficient laser desorption/ionization mass spectrometry (LDI-MS) of low molecular weight compounds *Analyst* **138** 7053–65
[14] Qian K, Zhou L, Liu J, Yang J, Xu H, Yu M, Nouwens A, Zou J, Monteiro M J and Yu C 2013 Laser engineered graphene paper for mass spectrometry imaging *Sci. Rep.* **3** 1415
[15] Liu C W, Chien M W, Su C Y, Chen H Y, Li L J and Lai C C 2012 Analysis of flavonoids by graphene-based surface-assisted laser desorption/ionization time-of-flight mass spectrometry *Analyst* **137** 5809–16
[16] Lin Z and Cai Z 2018 Negative ion laser desorption/ionization time-of-flight mass spectrometric analysis of small molecules by using nanostructured substrate as matrices *Mass Spectrom. Rev.* **37** 681–96
[17] Lu M, Lai Y, Chen G and Cai Z 2011 Laser desorption/ ionization on the layer of graphene nanoparticles coupled with mass spectrometry for characterization of polymers *Chem. Commun.* **47** 12807–9
[18] Kim Y K and Min D H 2015 The structural influence of graphene oxide on its fragmentation during laser desorption/ ionization mass spectrometry for efficient small-molecule analysis *Chem. Eur. J.* **21** 7217–23
[19] Wang D, Huang X, Li J, He B, Liu Q, Hu L and Jiang G 2018 3D printing of graphene-doped target for 'matrix-free' laser desorption/ionization mass spectrometry *Chem. Commun.* **54** 2723–6
[20] Lee G, Bae S-E, Huh S and Cha S 2015 Graphene oxide embedded sol–gel (GOSG) film as a SALDI MS substrate for robust metabolite fingerprinting *RSC Adv.* **5** 56455–9
[21] Reina G, González-Domínguez J M, Criado A, Vázquez E, Bianco A and Prato M 2017 Promises, facts and challenges for graphene in biomedical applications *Chem. Soc. Rev.* **46** 4400–16
[22] Criado A, Melchionna M, Marchesan S and Prato M 2015 The covalent functionalization of graphene on substrates *Angew. Chem., Int. Ed. Engl.* **54** 10734–50
[23] Quintana M, Vazquez E and Prato M 2013 Organic functionalization of graphene in dispersions *Acc. Chem. Res.* **46** 138–48
[24] Zhang W, Han H, Bai H, Tong W, Zhang Y, Ying W, Qin W and Qian X 2013 A highly efficient and visualized method for glycan enrichment by self-assembling pyrene derivative functionalized free graphene oxide *Anal. Chem.* **85** 2703–9
[25] Chen Y, Vedala H, Kotchey G P, Audfray A, Cecioni S, Imberty A, Vidal S and Star A 2012 Electronic detection of lectins using carbohydrate-functionalized nanostructures: graphene versus carbon nanotubes *ACS Nano* **6** 760–70
[26] Nair R R, Blake P, Grigorenko A N, Novoselov K S, Booth T J, Stauber T, Peres N M R and Geim A K 2008 Fine structure constant defines visual transparency of graphene *Science* **320** 1308
[27] Beloqui A, Calvo J, Serna S, Yan S, Wilson I B H, Martin-Lomas M and Reichardt N C 2013 Analysis of microarrays by MALDI-TOF MS *Angew. Chem., Int. Ed. Engl.* **52** 7477–81
[28] González-Domínguez J M, Santidrián A, Criado A, Hadad C, Kalbáč M and Da Ros T 2015 Multipurpose nature of rapid covalent functionalization on carbon nanotubes *Chem. Eur. J.* **21** 18631–41
[29] Serna S, Ercibengoa M, Marimón J M and Reichardt N C 2018 Measuring bacterial glycosyl hydrolase activity with a soluble capture probe by mass spectrometry *Anal. Chem.* **90** 12536–43
[30] Hos J 2019 On the suitability of raman spectroscopy to monitor the degree of graphene functionalization by diazonium salts *J. Phys. Chem.* C **123** 22397–402
[31] Zhang H, Bekyarova E, Huang J, Zhao Z, Bao W, Wang F, Haddon R C and Lau C N 2011 Aryl functionalization as a route to band gap engineering in single layer graphene devices *Nano Lett.* **11** 4047–51
[32] Hossain M Z, Walsh M A and Hersam M C 2010 Scanning tunneling microscopy, spectroscopy, and nanolithography of epitaxial graphene chemically modified with aryl moieties *J. Am. Chem. Soc.* **132** 15399–403
[33] Liu S J, Wen Q, Tang L J and Jiang J H 2012 Phospholipid-graphene nanoassembly as a fluorescence biosensor for sensitive detection of phospholipase D activity *Anal. Chem.* **84** 5944–50
[34] Cummings R D and Etzler M E 2009 Antibodies and lectins in glycan analysis *Essentials of Glycobiology* ed A Varki *et al* (New York: Cold Spring Harbor Laboratory Press) pp 1–25

[35] Echeverria B, Serna S, Achilli S, Vivès C, Pham J, Thépaut M, Hokke C H, Fieschi F and Reichardt N C 2018 Chemoenzymatic synthesis of N-glycan positional isomers and evidence for branch selective binding by monoclonal antibodies and human C-type lectin receptors *ACS Chem. Biol.* **13** 2269–79
[36] Brzezicka K, Echeverria B, Serna S, Van Diepen A, Hokke C H and Reichardt N C 2015 Synthesis and microarray-assisted binding studies of core xylose and fucose containing N-glycans *ACS Chem. Biol.* **10** 1290–302
[37] Ji D K, Zhang Y, He X P and Chen G R 2015 An insight into graphene oxide associated fluorogenic sensing of glycodye-lectin interactions *J. Mater. Chem.* B **3** 6656–61
[38] Chen Q, Wei W and Lin J M 2011 Homogeneous detection of concanavalin A using pyrene-conjugated maltose assembled graphene based on fluorescence resonance energy transfer *Biosens. Bioelectron.* **26** 4497–502
[39] Norton P, Comunale M A, Herrera H, Wang M, Houser J, Wimmerova M, Romano P R and Mehta A 2016 Development and application of a novel recombinant Aleuria aurantia lectin with enhanced core fucose binding for identification of glycoprotein biomarkers of hepatocellular carcinoma *Proteomics* **16** 3126–36
[40] Gray C J *et al* 2017 Label-free discovery array platform for the characterization of glycan binding proteins and glycoproteins *Anal. Chem.* **89** 4444–51
[41] Fukumori F, Takeuchi N, Hagiwara T, Ohbayashi H, Endo T, Kochibe N, Nagata Y and Kobata A 1990 Primary structure of a fucose-specific lectin obtained from a mushroom, Aleuria aurantia *J. Biochem.* **107** 190–6
[42] Hu J, Liu F and Ju H 2016 MALDI-MS patterning of caspase activities and its application in the assessment of drug resistance *Angew. Chem., Int. Ed. Engl.* **55** 6667–70